Eur. Phys. J. A **46**, 329–336 (2010)
DOI 10.1140/epja/i2010-11052-7

THE EUROPEAN PHYSICAL JOURNAL A

Regular Article – Experimental Physics

In-beam measurements of sub-nanosecond nuclear lifetimes with a mixed array of HPGe and $LaBr_3$:Ce detectors

N. Mărginean[1], D.L. Balabanski[2], D. Bucurescu[1,a], S. Lalkovski[3], L. Atanasova[2], G. Cătа-Danil[1], I. Cătа-Danil[1], J.M. Daugas[4], D. Deleanu[1], P. Detistov[2], G. Deyanova[3], D. Filipescu[1], G. Georgiev[5], D. Ghiţă[1], K.A. Gladnishki[3], R. Lozeva[5], T. Glodariu[1], M. Ivaşcu[1], S. Kisyov[3], C. Mihai[1], R. Mărginean[1], A. Negret[1], S. Pascu[1], D. Radulov[3], T. Sava[1], L. Stroe[1], G. Suliman[1], and N.V. Zamfir[1]

[1] Horia Hulubei National Institute of Physics and Nuclear Engineering (IFIN-HH), R-76900 Bucharest, Romania
[2] Institute for Nuclear Research and Nuclear Energy (INRNE), Bulgarian Academy of Sciences, Sofia, Bulgaria
[3] St. Kliment Ohridski University, Sofia, Bulgaria
[4] CEA, DAM, DIF, F-91297 Arpajon, France
[5] CSNSM, F-91404 Orsay, France

Received: 16 June 2010 / Revised: 13 September 2010
Published online: 24 October 2010 –
Communicated by C. Signorini

Abstract. A fast-timing method to determine lifetimes of nuclear states in the sub-nanosecond domain is presented. It is based on in-beam measurements of triple-gamma coincidences in heavy-ion fusion-evaporation reactions, performed with an array of HPGe and $LaBr_3$:Ce detectors. The high-energy resolution HPGe detectors are used to define de-exciting cascades, while the fast $LaBr_3$:Ce detectors are used to determine the decay time spectra of selected levels fed by these cascades. A special method to treat the time information of an array of fast detectors is employed in order to fully use the efficiency of the array. Two measurements are presented to illustrate the method: a re-determination of the known half-life $T_{1/2} = 0.7$ ns of the $E_x = 205$ keV, $J^\pi = 7/2^+$ level in ^{107}Cd (test experiment), and the determination of a half-life $T_{1/2} = 47$ ps for the $E_x = 367$ keV, $J^\pi = 3/2^+$ state of ^{199}Tl.

1 Introduction

The measurement of lifetimes of excited nuclear states is one of the most important topics in nuclear spectroscopy because these quantities are the essential ingredient in the determination of the reduced electromagnetic transition probabilities, that are rather sensitive to details of the intrinsic structure of these states. The lifetimes encountered at low and medium nuclear excitations cover many orders of magnitude and consequently there are several specific methods of measurement each covering a certain range [1]. Among these, the electronic method, based on the direct measurement of the time decay spectrum of a certain state, is based on the use of fast detectors (with good timing properties), such as certain scintillators, and appropriate electronics. This method continuously benefited from the occurence of new scintillators and is currently applicable to lifetimes down to a few picoseconds. Thus, based on the use of the BaF_2 crystals, the capabilities of the delayed coincidence method were pushed into the low-picosecond range. This method, designed for use in the β-decay, employs triple-$\beta\gamma\gamma$ coincidence measurements and is suitable especially for the investigation of the neutron-rich nuclei where it was applied in many cases ([2–4] and references therein). One of the γ-ray detectors is a Ge detector, and its good energy resolution is used to select the desired decay branch. The other two detectors are the timing detectors: a thin scintillator for the β-rays, and a BaF_2 one for the γ-rays.

The γ-ray spectroscopy in fusion-evaporation reactions allows the population of many more nuclear states. However, the use of a similar method for $\gamma\gamma\gamma$ delayed coincidence measurements, in which one of the detectors is a Ge and the other two are scintillators (with good timing properties) could not be used in the past due to the large number of γ-rays in the spectra and the poor energy resolution of the BaF_2 detectors. The occurence of new scintillators, such as $LaBr_3$:Ce, is about to change this situation. These new detectors have excellent properties concerning time resolution (100 to 300 ps depending on the crystal size), energy resolution (typically 2–3% at 662 keV), high efficiency and light output per keV (more than 63 photons per keV), and fast decay time ($\sim$ 16 ns) [5–7]. The use of a $LaBr_3$:Ce detector, but again in $\beta\gamma\gamma$ measurements,

[a] e-mail: bucurescu@tandem.nipne.ro

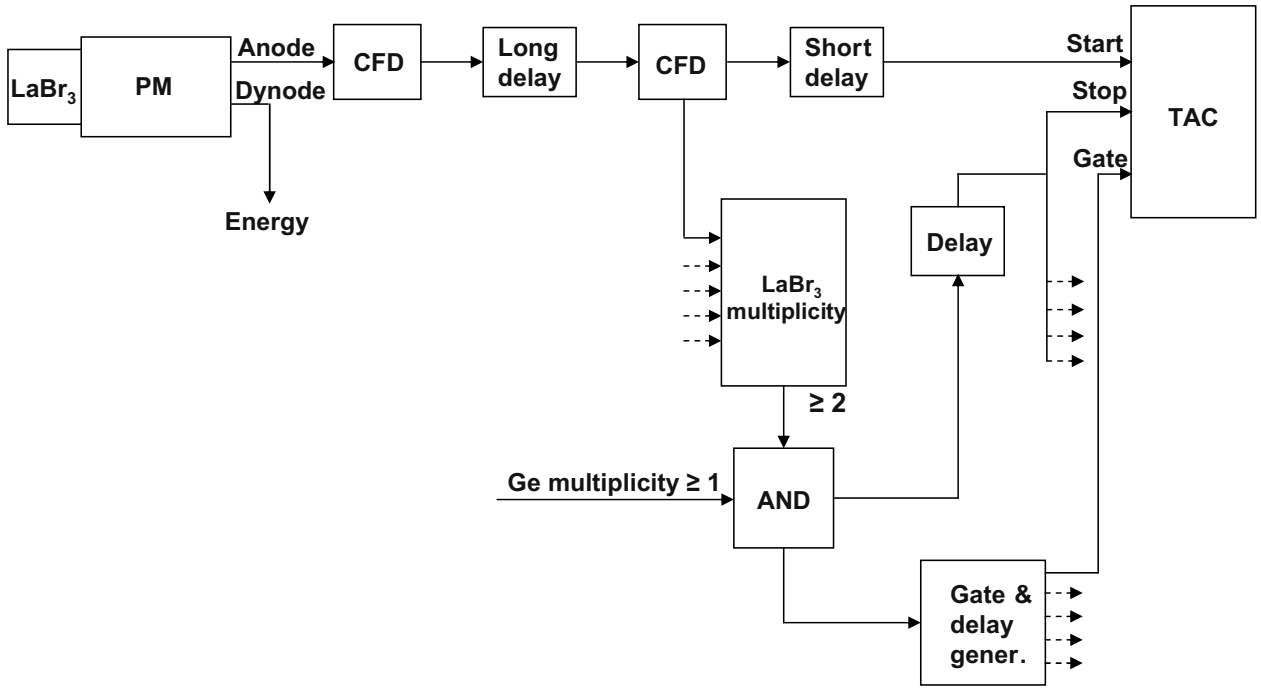

Fig. 1. Part of the electronic scheme detailing the timing processing for one of the five $LaBr_3$:Ce detectors.

was recently reported for the determination of lifetimes of high-spin states in ^{122}Cd populated in the β-decay of a (9^-) isomer of ^{122}Ag [8].

In this work we present a development of the fast-timing method which is suitable for in-beam γ-ray spectroscopy measurements. Triple-gamma coincidences are measured with an array containing both HPGe and $LaBr_3$:Ce detectors. The high-energy resolution of the Ge detectors is used to select the desired γ-ray cascade, and the array of fast $LaBr_3$:Ce to build the delayed coincidence time spectra for selected levels. In order to fully use the efficiency of the $LaBr_3$:Ce array, that is, all $\gamma\gamma$ coincidence combinations between these detectors, a special method is necessary for the processing of the time information from the $LaBr_3$:Ce detectors, and this is presented in some details. The method is illustrated by two in-beam level lifetime measurements, one in ^{107}Cd, populated with the ^{98}Mo(^{12}C, 3nγ) reaction, and the other in ^{199}Tl, following the ^{197}Au(α, 2nγ) reaction.

2 Experiment arrangement

The measurements were performed with beams delivered by the Tandem van de Graaff accelerator in Bucharest. In the first experiment, a 1.3 mg/cm^2 ^{98}Mo target with a 29.5 μm Pb backing was bombarded with a 50 MeV ^{12}C beam with intensity of about 10 pnA. In the second experiment, a 9.65 mg/cm^2 Au foil was bombarded by a 24 MeV α-particle beam with intensity around 10 nA. The detection of the γ-rays was made with 7 HPGe detectors each with relative efficiency around 50%, five of them being placed at 143° and the other two at 90° with respect to the beam, and five $LaBr_3$:Ce detectors placed at 45° with respect to the beam. The $LaBr_3$:Ce detectors, delivered by Saint-Gobain Crystals, had crystals of $2'' \times 2''$ (one), $1.5'' \times 1.5''$ (two), and $1'' \times 1''$ (two) and photomultipliers XP5500B. Energy and efficiency calibrations of the detectors were performed with standard sources of ^{60}Co, ^{137}Cs, and ^{152}Eu. Coincidences between all these 12 detectors were registered on-line and processed after the experiments. The energy information of the detectors was treated by conventional amplification chains.

Figure 1 shows details of the electronics that are relevant for the $LaBr_3$:Ce detectors and the treatment of their time information. For each $LaBr_3$:Ce detector we have used the anode signal for the timing, and the signal from the last dynode for the energy information. Although this non-standard choice does not ensure the optimum timing signals, we used the weakest signal for the energy chain such that one does not rapidly reach the saturation (because of the large light output). For each detector we have chosen the high voltage at which the best linearity in energy was achieved, which simplified the off-line energy alignment of the different detectors. The timing signals were passed first through constant fraction discriminator modules (type ORTEC 935) —fig. 1. Because the Ge detectors are much slower than the $LaBr_3$:Ce ones, the signals from these CFDs had to be delayed by about 500 ns, and this was done by using only long cables, avoiding additional electronic time jitter. Then, the signals were passed again through CFDs to rebuild their front. From these CFDs, one signal, appropriately delayed for synchronization (by a short delay) was sent as start signal of a time-to-amplitude converter (TAC). The other signal from CFD was sent to a coincidence/multiplicity unit. The resulting

signals with multiplicity equal to or larger than 2 were fed into another coincidence unit where the trigger signal of the experiment was built from an "and" operation with the multiplicity one signal separately built for the germanium detectors. This trigger signal was used, on one hand, to generate a gate signal for the TACs such as to reduce their load. On the other hand, because the front of this signal was given by the $LaBr_3$:Ce detector multiplicity signal, it could be distributed as a "common" stop signal to all the TAC units. This was done again only by cabling, therefore avoiding additional jitter. In this way, exactly the same stop was used for all TACs, and in the off-line analysis the time differences between different detectors do not affect the time resolution.

Because we finally look at time differences of pairs of $LaBr_3$:Ce detectors, it is of utmost importance to properly treat the time information from the detectors, in order to be able to add up the contributions from all pairs of detectors. The following off-line processing procedure was adopted. A ^{60}Co source was placed precisely at the position of the beam spot. The ^{60}Co source represents a perfect case of prompt coincidence between two γ-rays. One chooses one of the scintillator detectors as a time reference (therefore only events of fold two and containing signal from that detector are chosen). Then, for each of the rest of scintillator detectors one builds a matrix $E_\gamma \Delta T$, where ΔT is the time difference with respect to the reference detector, and a gate was set on the 1332 keV transition in the reference detector. In this way one gets the response of the CFD as a function of energy, for all energies smaller than 1173 keV. Such a time response is shown in fig. 2(a) for a certain pair of detectors (the $2'' \times 2''$ detector refered to one of the $1.5'' \times 1.5''$ detectors). One observes a non-linear dependence of the time response on the energy (a time walk), that was found to be independent of the detector chosen as a reference, therefore it represents the instrumental time response for that detector —CFD combination. Different detectors will have different such time walks, which would make it impossible to combine the time information from all of them. Therefore, for each such matrix one fits the average energy dependence of the time response with a polynomial function. This function was composed of polynomials up to the second order, separately applied on successive energy domains and smoothly joined between them. Then, by using this function one corrects the time response of that detector such that one completely removes the energy dependence, leading to an optimum time resolution (fig. 2(b)). This is equivalent to the alignment of the time response for any energy to the position of the prompt full-energy peak coincidence 1173-1332 keV, which is very precisely defined (fig. 2). This procedure is repeated for all detectors, therefore resulting in a perfect time alignment of all pairs of detectors. The time calibration of the spectra was performed with a standard time calibrator. The range of the TACs was of 50 ns. Typical time resolutions (FWHM, for the ^{60}Co source peak-to-peak coincidences) were about 150 ps for the small ($1'' \times 1''$) detectors, about 180 ps for the middle-size ($1.5'' \times 1.5''$) ones, and about

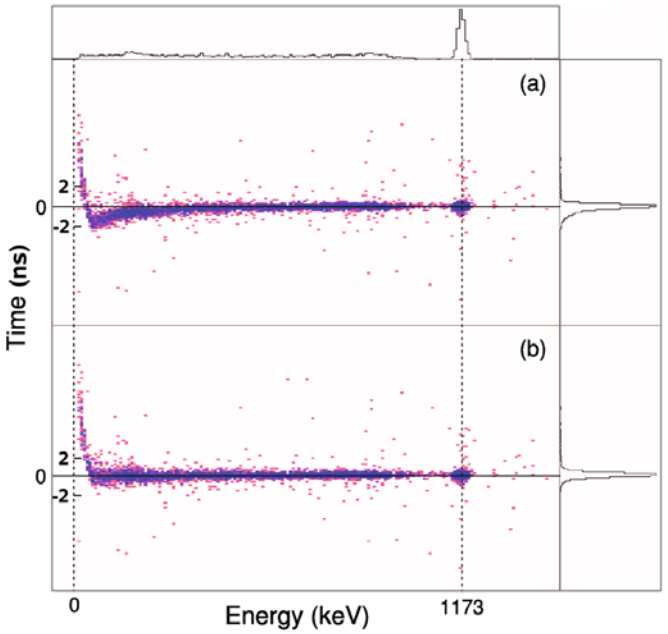

Fig. 2. Example of time walk correction to the $LaBr_3$:Ce detectors. (a) Time difference —energy matrix having as start one of the $1.5'' \times 1.5''$ $LaBr_3$:Ce detectors, and as stop the largest ($2'' \times 2''$) $LaBr_3$:Ce detector, measured with a ^{60}Co source placed in the target position, and gated by the 1332 keV transition. (b) The same matrix after applying the time walk correction as described in the text. Note that the correction was not applied at the lowest energies, which were outside the range of interest.

300 ps for the largest ($2'' \times 2''$) one. One should note that the alignment of the time signals is independent of this time resolution, and its accuracy is that of the centroid of the prompt coincidence, that is, a fraction of one channel (fitting a polynomial curve to the time response and then correcting for the determined variation with the energy is equivalent to the procedure of aligning the energy gain of two detectors by matching their peak centroids) —which in our case (fig. 2) is of the order of 5 ps.

After all these corrections, a $E_{\gamma_1} E_{\gamma_2} \Delta t$ coincidence cube was built for the $LaBr_3$:Ce detector coincidences, using all the data. We briefly describe how this cube is constructed. Assume that a double-$\gamma\gamma$ coincidence event is recorded, consisting of γ-ray number 1 (γ_1) detected by the detector number i and γ-ray number 2 (γ_2) detected by the detector number j (with i, j being any of the numbers between 1 and 5). The projection in the energy plane will be a symmetric $E_{\gamma_1} E_{\gamma_2}$-matrix constructed in the usual mode, that is, we record one event in the $x = E(\gamma_1)$, $y = E(\gamma_2)$ position, and a second one in the $x = E(\gamma_2)$, $y = E(\gamma_1)$ position. The time difference for the first event is recorded as $\Delta t + T$, where $\Delta t = t_{1,i} - t_{2,j}$ and T is an arbitrary offset (channel). For the second event a time difference $-\Delta t + T$ is recorded. In this way, the two axes are distinguished, with the x-axis assuming, say, the role of "start" axis, and the y-axis the one of "stop" axis, respectively.

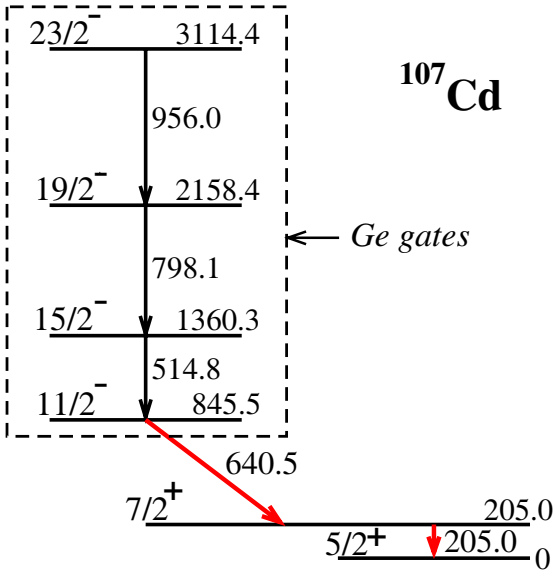

Fig. 3. Relevant part of the level scheme of ^{107}Cd [9]. The dashed rectangle comprises the three transitions used for gating in the HPGe detector spectra.

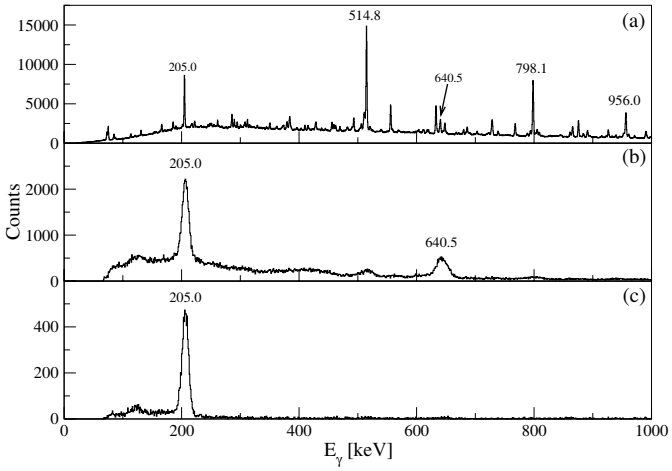

Fig. 4. (a) Projection of the HPGe axis of a $\gamma\gamma\gamma$ (HPGe-$LaBr_3$-$LaBr_3$) coincidence cube; (b) the energy projection of a $E_\gamma E_\gamma \Delta t$ cube constructed for the $LaBr_3$:Ce detectors, gated by the transitions 515, 798, and 956 keV detected in the HPGe detectors (highlighted in fig. 3); (c) gate on the 640.5 keV transition in spectrum (b), obtained from the $\gamma\gamma$ coincidence ($LaBr_3$-$LaBr_3$) matrix projected from the cube described at (b).

3 Measurements

3.1 Test measurement: the lifetime of the 205 keV state of ^{107}Cd

States in ^{107}Cd were populated in the ^{98}Mo(^{12}C, 3n)^{107}Cd reaction at 50 MeV beam energy. Figure 3 shows the relevant part of the level scheme [9]. Different matrices and cubes were sorted out from the $\gamma\gamma\gamma$ coincidences. Figure 4(a) shows the Ge-energy axis projection of a $\gamma\gamma\gamma$ cube. By gating on this axis on the strong yrast transitions of 956, 798, and 515 keV in this spectrum, one selects the 640-205 keV decay sequence (fig. 2) in the $LaBr_3$:Ce detectors, which contains the $7/2^+$ level of interest. The two transitions can be seen in fig. 4(b), while the spectrum in fig. 4(c) shows the scintillator spectrum gated by both the Ge detectors (yrast transitions above the $11/2^-$ states) and the 640 keV transition detected in the scintillators. Figure 5(a) shows the resulting delayed coincidence time spectrum for the 205 keV transition, resulted from gating on the two γ-rays on an energy-energy time difference $\gamma\gamma\Delta T$ cube constructed for the $LaBr_3$:Ce detectors gated by the HPGe detectors. This is the typical time-delayed spectrum, obtained when the start was given by the transition above the level (640 keV in our case) and the stop by the transition de-exciting the level (205 keV in our case), respectively (cf. the discussion above about the "start" and "stop" axes). It clearly shows an exponential tail due to a decay time larger than the width of the prompt coincidence spectrum. The exponential decay $e^{-t/\tau}$ was convoluted with a Gaussian obtained by fitting the prompt coincidence peak (determined by gating on the Compton background near the 205 keV peak), and the fit to the experimental data (continuous line) provides a value $T_{1/2} = 0.69 \pm 0.03$ ns, which agrees, within uncertainties,

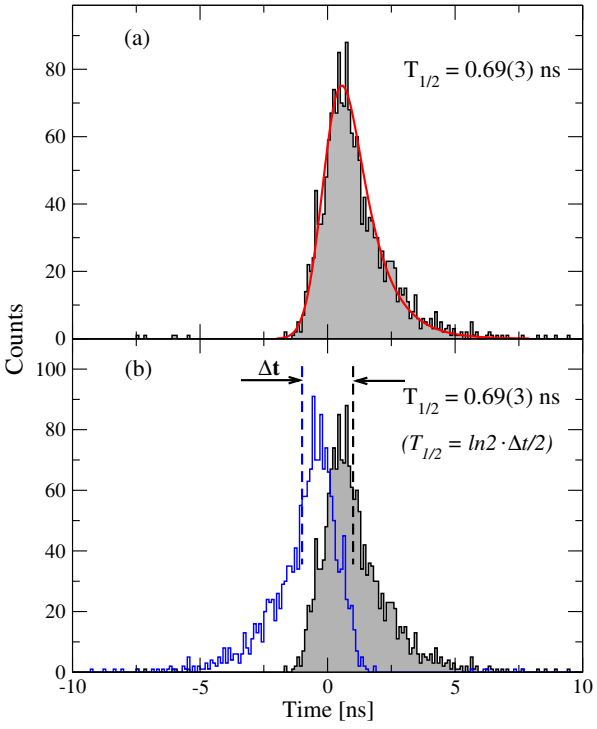

Fig. 5. (a) Delayed coincidence time spectrum of the 205.0 keV level. The continuous line is a fit to the data with an exponential decay convoluted with a Gaussian representing the prompt coincidence time spectrum, that provides a half-life of 0.69 ± 0.03 ns. (b) Delayed coincidence time spectra obtained for the 205.0 keV level with two alternatives: i) start with the 640.5 keV transition and stop with the 205.0 keV one (this is identical with the spectrum shown in (a)); ii) start with the 205.0 keV transition and stop with the 640.5 keV one (see fig. 3). The dashed lines indicate the centroids of the two distributions, their time difference being twice the lifetime of the level.

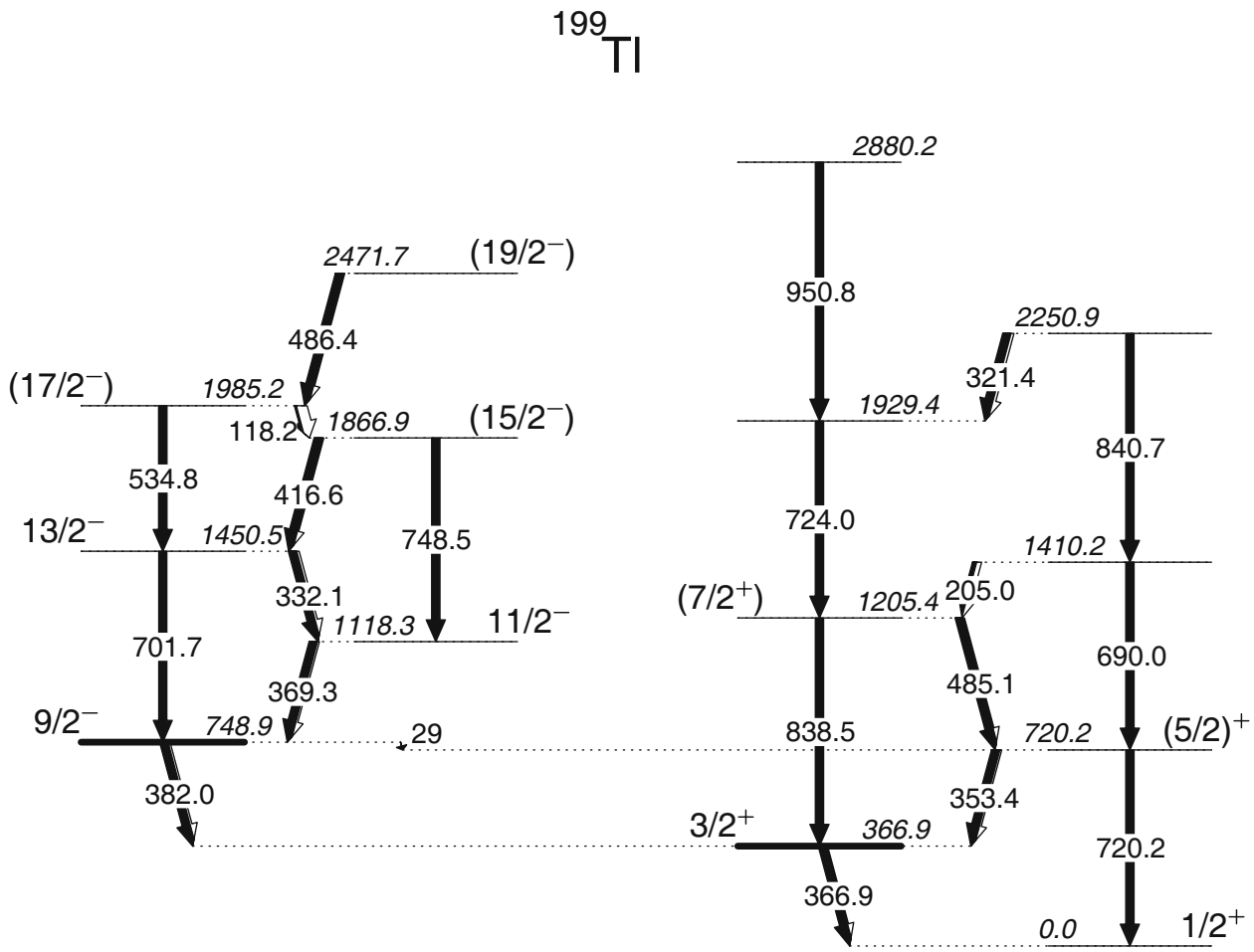

Fig. 6. Relevant part of the level and decay scheme of ^{199}Tl as seen in this experiment. The level at 748.9 keV is a known isomer with a half-life of 28.4 ms [11].

with the ENSDF adopted value of $T_{1/2} = 0.71 \pm 0.04$ ns [9]. In this fit we have chosen the zero-time channel as that taken for the numerical offset value, but, in principle, the zero time can be also taken as a free parameter. Figure 5(b) illustrates an alternative determination of this lifetime. One can obtain the decay curve symmetric to that in fig. 5(a) by using the 205 keV transition as start and the 640 keV transition as stop. The time difference Δt between the centroids (first-order moments) of the two decay distributions is twice the lifetime τ. The determined $T_{1/2}$ value coincides with the one obtained with the fit in fig. 5(a). This centroid method is obviously the one to use when the time resolution is comparable to, or larger than, the lifetime being measured. One should note that the two time distributions are not perfectly symmetric (there are small differences, of 1–2 counts per channel) because of rounding errors in calculating the coordinates of the areas used to define the background subtraction.

3.2 Lifetime of the 367 keV state of ^{199}Tl

The Tl isotopes with $N \leq 126$ have $1/2^+$ ground state and a low-lying $3/2^+$ excited state. In ^{207}Tl, the two states are almost pure $s_{1/2}$ and $d_{3/2}$ proton-hole states, respectively, in the ^{208}Pb doubly magic core, and the single-particle character of the $3/2^+ \rightarrow 1/2^+$ transition results in a rather long lifetime of the $3/2^+$ state, $T_{1/2} = 30(7)$ ps, and a $B(E2)$ value of 2.7(6) W.u. [10]. With decreasing number of neutrons, this transition increases in collectivity ($B(E2)$ increases) up to ^{201}Tl, the lifetime of this state remaining in the range tens of ps to 1.5 ns [10]. In ^{199}Tl the lifetime of the $3/2^+$ state is not accurately known ($T_{1/2} < 1.5$ ns [11]), and, according to this systematics, we expected that it is in the range of tens to hundreds of ps, therefore a good test for the capability of our measuring method.

States in ^{199}Tl were populated with the ^{197}Au$(\alpha, 2n)^{199}$Tl reaction at 24 MeV beam energy. Figure 6 shows the relevant level scheme populated in this reaction [11–13]. From the analysis of the $\gamma\gamma$ coincidences recorded in the HPGe detectors, we were able to significantly develop the level scheme proposed in the earlier (α,2n) reaction studies [12,13]. Nevertheless, as in this paper we concentrate on the methods to measure sub-nanosecond lifetimes, the newly developed level scheme will be published separately. In fig. 6 we show only a few new transitions added to the two band

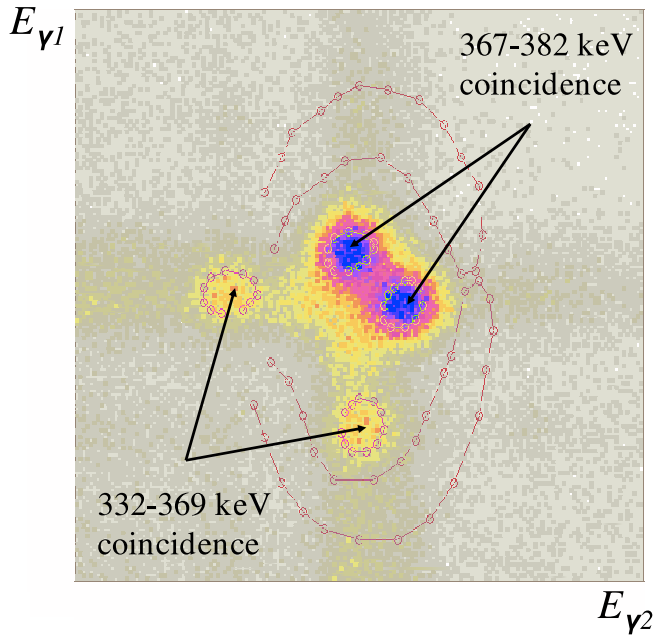

Fig. 7. Relevant part of the symmetric $\gamma\gamma$ coincidence ($LaBr_3$-$LaBr_3$) matrix obtained as a projection of the $E_{\gamma 1}E_{\gamma 2}\Delta t$ cube described in the text. It shows the coincidence relationships between the two pairs of γ-rays, 332 and 369 keV above the 748.9 long-living isomer, and 382 and 367 keV below this isomer, this later pair of transitions framing the level of interest. The full line contours that link open circles are the peak gates and the background bananas.

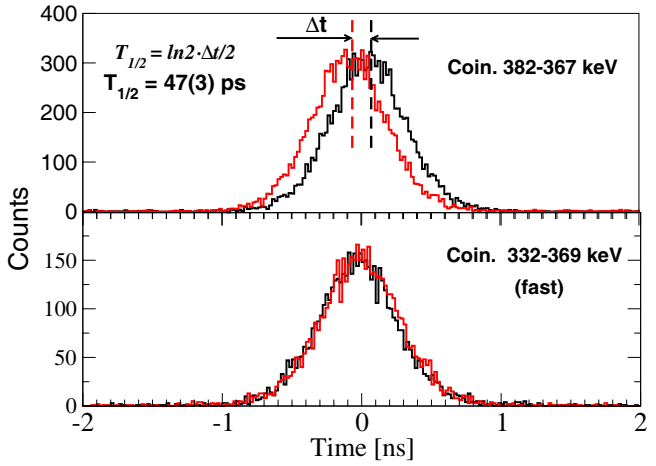

Fig. 8. Time spectra for the pair of γ-ray transitions 382-367 keV (top graph), and 332-369 keV (bottom graph). The two time distributions in each case were obtained by gating on the two transitions as start and stop in both possible ways. The bottom spectrum corresponds to a "prompt" coincidence, the 1118.3 keV level (fig. 6) having a short lifetime, indiscernible with the present method, while the top spectrum shows a clear shift of the centroid (first-order momentum of the distribution), corresponding to the lifetime of the 367 keV level, as indicated.

structures built on the $1/2^+$ and $3/2^+$ states, respectively, above the $(7/2^+)$ level at 1205 keV.

Figure 7 shows a part of the two-dimensional energy projection of a the $E_\gamma E_\gamma \Delta T$ coincidence cube for the $LaBr_3$:Ce detectors. This matrix was no longer gated by the Ge detectors, because pairs of coincident γ-rays of interest appear very clearly. This matrix was constructed with the start energy signals on one axis, and the stop signals on the other axis (as discussed in the previous section). One can clearly see four peaks, representing the pairs of coincidences 332-369 keV, and 382-367 keV, respectively. Incidentally, one should remark the good energy resolution of the $LaBr_3$:Ce detectors that allows a good separation of a 15 keV doublet. This is also a very good case for testing our time alignment procedure, because we have two pairs of gammas of comparable energies, but with different time characteristics. The first pair of coincidences should represent a "prompt" coincidence, since it contains transitions that feed/decay the 1118 keV state (which has a short lifetime), while the second one contains the feeding/decay of the 367 keV state, which might show a delayed coincidence, characterized by the lifetime of the $E_x = 367$ keV state. Time spectra obtained by gating on these pairs of γ-rays are shown in fig. 8. In each case two time spectra are presented, one obtained by gating on the γ-ray above the level as a start transition and on the γ-ray below the level as a stop transition, and the second with inverted roles for the two transitions. One can see that in the first case (the 332-369 keV coincidence) the time spectra thus obtained are practically identical, representing indeed a prompt coincidence (of overall FWHM = 670 ps), while in the 382-367 keV case the two time peaks have displaced centroids, due to a lifetime of the 367 keV level which is shorter than the time resolution of the prompt coincidence peak. The difference between the centroids of the two peaks is obviously twice the lifetime of the 367 keV state, resulting in a value $T_{1/2} = 47 \pm 3$ ps. This measurement shows that with such a setup with 5 scintillator detectors one can easily measure lifetimes of the order of a few tens of picoseconds. The quoted error represents only the contribution of the statistical error in determining the centroid (first-order moment) of the distribution. For the same level, at $E_x = 367$ keV, we have tested also the time distribution obtained on the basis of the 838-367 keV coincidence (fig. 6). We found a similar displacement of the centroid, which confirms a lifetime compatible with the value given above, but in this case the statistic was much lower (note that the thicknesses of the transition arrows in fig. 6 do not represent γ-ray intensities).

Using this lifetime, and the mixing ratio and internal conversion coefficient of the 367 keV transition as given in [11], we calculated the reduced transition probabilities $B(E2)$ and $B(M1)$ for this transition, of 16.6(1.7) and 0.0023(3) W.u., respectively. These values are compared to the similar ones in the heavier isotopes 201 to 207 in fig. 9. One can see that the values determined with the present measurement continue the relatively smooth evolution with mass, indicating an increase in the collectivity of the $3/2^+$ state (slightly larger $B(E2)$ values) with decreasing mass.

The centroid shift method analysis presented above deserves some further discussion. The difference between the

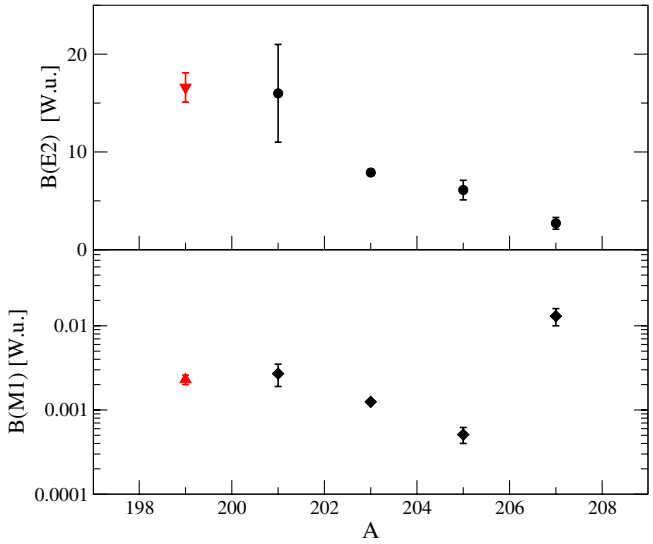

Fig. 9. Systematics of the $B(\sigma\lambda)$ values for the $3/2^+ \rightarrow 1/2^+$ transition in the odd-mass Tl isotopes with mass 199 to 207. The values for ^{199}Tl correspond to the lifetime determined in the present work, and the mixing ratio and internal conversion coefficient of the 367 keV transition as given in ref. [11].

centroids of the two time distributions is exactly twice the level lifetime if the prompt coincidence spectrum distribution (which convolutes the exponential decay) has a symmetrical shape (*e.g.*, a Gaussian, as seen in fig. 8). In our case this is true for any pair of detectors due to i) the time walk correction, which eliminates the energy-dependent asymmetries in the time response, and ii) the careful time alignment of the detectors with the ^{60}Co source placed in the same emission point as in the in-beam experiment, which eliminates any geometrical path difference and implicitly angular-distribution effects.

Another aspect concerns the possible systematic error in the centroid difference that would occur due to subtraction of the prompt coincidence background. This type of error is considerably reduced in our case, because we avoid as much as possible subtraction procedures by using more reliable selection methods that greatly reduce the background, such as the coincidence with the HPGe detectors (selection of the cascade) and two-dimensional ("circular") energy gating.

It is not straightforward to estimate a lower limit for the lifetimes measured by this approach. In this experiment, a half-life value of 47 ps was measured, which is much lower than the overall resolution of the prompt coincidence peak. How much lower one can go depends also to a large extent on the statistics of the measurement, which determines the error of the extracted centroids. One may compare this capability with that demonstrated by the Doppler shift attenuation measurements with very low-velocity reactions, such as $(p, n\gamma)$ or $(n, n'\gamma)$, where centroid shifts of γ-ray peaks are measured that are very much lower than the energy resolution of the detector. In the 10–20 ps range the TAC conversion limitations and the electronics stability should have an important influence. Further experiments will show the real limitations of the method. What is important for the time being is that the presently developed method can be confortably used in in-beam measurements of lifetime values within a range that overlaps well with that of another in-beam method, the recoil-distance (plunger) method.

4 Conclusions

In the present work we demonstrated the feasibility of nuclear lifetime measurements in the sub-nanosecond domain in fusion-evaporation reactions by the fast-timing method. The method employed uses triple-$\gamma\gamma\gamma$ coincidences of a mixed array of HPGe and $LaBr_3$:Ce detectors. The good energy resolution HPGe detectors are used to gate on γ-rays or cascades that feed the levels of interest, while both the fast timing and good energy resolution properties of the $LaBr_3$:Ce scintillators are used to generate the delayed coincidence spectra. We describe a method that allows to fully use the efficiency of the scintillator array by providing the possibility to combine the time spectra from all $LaBr_3$:Ce detector pairs. The method was first tested by confirming the known 0.7 ns half-life of the 205 keV, $7/2^+$ state in ^{107}Cd, and then used to measure, for the first time, a half-life of 47 ps for the 367 keV, $3/2^+$ level in ^{199}Tl.

The method developed in this work allows an extension of the application of the fast-timing method to *in-beam* measurements, such as the fusion-evaporation or fragmentation reactions, where the number of the open channels and consequently of the γ-rays in the spectra may be rather large. It was demonstrated that the method can be used down to the lifetime range of tens of picosends, which overlaps well with that of the plunger method.

This work was partly supported by the Romanian Ministry for Education and Research under the research projects 71-042/2007, 24EU-ISOLDE/2009, IDEI-118/2007, IDEI-48/2007, IDEI-181/2007, and PN 09370105/2009, and by the Bulgarian National Science Fund, under contracts DID-02/16, DNFK-02/5, BRS-03/07, and EC FP7 SP2PP(212693).

References

1. T.K. Alexander, J.S. Foster, *Advances in Nuclear Physics*, edited by M. Baranger, E. Vogt, Vol. **10** (Plenum Press, New York, London, 1978) p. 197.
2. H. Mach, R.L. Gill, M. Moszyński, Nucl. Instrum. Methods Phys. Res. A **280**, 49 (1989).
3. M. Moszyński, H. Mach, Nucl. Instrum. Methods Phys. Res. A **277**, 407 (1989).
4. H. Mach, F.K. Wohn, G. Molnár, K. Sistemich, J.C. Hill, M. Moszyński, R.L. Gill, W. Krips, D.S. Brenner, Nucl. Phys. A **523**, 197 (1991).
5. I.K. Mackenzie, Nucl. Instrum. Methods Phys. Res. A **299**, 377 (1990).
6. E.V.D. van Loef, P. Dorenbos, C.W.E. van Eijk, K.W. Kramer, H.U. Güdel, Nucl. Instrum. Methods Phys. Res. A **486**, 254 (2002).

7. D. Alexiev, D.A. Prokopovich, M.L. Smith, M. Matuchova, IEEE Trans. Nucl. Sci. **55**, 1174 (2008).
8. D.L. Smith, H. Mach, H. Pentilä, H. Bradley, J. Äystö, V.-V. Elomaa, T. Eronen, D.G. Ghiţă, J. Hakala, M. Hauth, A. Jokinen, P. Karvonen, T. Kessler, W. Kurcewicz, H. Lehmann, I.D. Moore, J. Nyberg, S. Rahaman, J. Rissanen, J. Ronkainen, P. Ronkanen, A. Saastaminen, T. Sonoda, O. Steczkiewicz, C. Weber, Phys. Rev. C **77**, 014309 (2008).
9. J. Blachot, Nucl. Data Sheets **109**, 183 (2008).
10. Evaluated Nuclear Structure Data File (ENSDF), maintained by the National Nuclear Data Center, Brookhaven National Laboratory (`http://www.nndc.bnl.gov/ensdf`).
11. B. Singh, Nucl. Data Sheets **108**, 79 (2007).
12. J.O. Newton, S.D. Cirilov, F.S.Stephens, R.M. Diamond, Nucl. Phys. A **148**, 593 (1970).
13. Liu Fengying, Wen Shuxian, Han Benhua, Weng Peikun, Yang Chunxiang, Chin. J. Nucl. Phys. **8**, 305 (1986).